Chapter 9
Catchment-Scale Natural Water Balance in Chile

Nicolás Vásquez, Javier Cepeda, Tomás Gómez, Pablo A. Mendoza, Miguel Lagos, Juan Pablo Boisier, Camila Álvarez-Garretón, and Ximena Vargas

Abstract Characterizing the temporal evolution of water storages and fluxes over large domains can not only help to improve understanding on the interplay between physical controls, climate and hydrological behavior, but also to inform water management decisions. In this chapter, a historical context, the methodology and catchment-scale results for ongoing efforts to characterize the natural water balance in Chile are provided. To this end, the Variable Infiltration Capacity (VIC) hydrological model is run using gridded meteorological forcings estimated from in-situ observations and reanalysis data. Details on the criteria for selecting near-natural catchments, the collection and generation of datasets, and hydrological model descriptions are provided. The main insights on the annual and seasonal water balances across the study domain and perspectives for future work are discussed.

N. Vásquez · J. Cepeda · T. Gómez · X. Vargas (✉)
Departamento de Ingeniería Civil, Facultad de Ciencias Físicas y Matemáticas, Universidad de Chile, Santiago, Chile
e-mail: xvargas@uchile.cl

P. A. Mendoza · M. Lagos
Departamento de Ingeniería Civil, Facultad de Ciencias Físicas y Matemáticas, Universidad de Chile, Santiago, Chile

AMTC, Centro Avanzado de Tecnología para la Minería, Facultad de Ciencias Físicas y Matemáticas, Universidad de Chile, Santiago, Chile

J. P. Boisier
CR-2, Centro de Ciencia del Clima y la Resiliencia, Santiago, Chile

Departamento de Geofísica, Facultad de Ciencias Físicas y Matemáticas, Universidad de Chile, Santiago, Chile

C. Álvarez-Garretón
CR-2, Centro de Ciencia del Clima y la Resiliencia, Santiago, Chile

Instituto de Conservación, Biodiversidad y Territorio, Universidad Austral de Chile, Valdivia, Chile

B. Fernández, J. Gironás (eds.), *Water Resources of Chile*, World Water Resources tba2, https://doi.org/10.1007/978-3-030-56901-3_9

Keywords Water balance · Catchment · Infiltration · VIC · Gridded data · Meteorology · Runoff

9.1 Introduction

The natural availability of water resources at the catchment scale depends on complex interactions of water and energy fluxes and storages at a range of spatiotemporal scales. Given the growing water demands from different sectors – associated to increased global population – and changing climatic conditions due to natural variability and anthropogenic forcings (e.g., Milly et al. 2005, 2008; Huntington 2006; IPCC 2013), there is an imperative need for accurate water balance estimations to inform management decisions.

A key challenge for such estimates is the scarcity of ground measurements (including hydro-meteorological variables, physical properties and water-use) to represent natural systems. This is a critical issue in Chile, where topography is complex, and both economy and population are highly-centralized (40% of the latter is spanned over 2% of the country's area). Given the lack of an adequate observational network, modeling techniques are required to estimate water balance components across the complete domain (Müller Schmied et al. 2016), a task challenged by many sources of uncertainty.

9.1.1 Modeling the Water Balance at the Catchment Scale

The urgency to quantify natural water resources has motivated water balance studies worldwide, spanning from the regional to the global scale. While some efforts have focused on the partitioning of annual precipitation into runoff and evapotranspiration (e.g., Sankarasubramanian and Vogel 2002; Carmona et al. 2014; Mizukami et al. 2016), others have aimed to provide seasonal characterizations (e.g., Vandewiele and Elias 1995; Martinez and Gupta 2010; Berghuijs et al. 2014), or even daily (e.g., Parajka et al. 2007; Tian et al. 2017) water balance estimates. A common path forward is the use of large samples of catchments to learn from diversity (e.g., Sivapalan 2018), practice referred to as large-sample hydrology (Andréassian et al. 2006; Gupta et al. 2014). In particular, large-sample hydrology can help to understand the interplay between physical similarity (e.g., topographic descriptors, land cover characteristics), climatic similarity, and hydrologic similarity, with the aim to develop techniques to address the problem of prediction in ungagged basins (PUB; see review by Hrachowitz et al. 2013).

Although many authors have stressed the need to understand, quantify and reduce hydrologic uncertainty in a changing world (Addor et al. 2014; Mendoza et al. 2016; Clark et al. 2016), improving process understanding under current climatic conditions is a critical first step (e.g., Blöschl and Montanari 2010). Over the past decades, many water balance studies have benefited from advances in process-based hydrological models (e.g., Wigmosta et al. 1994; Chen et al. 1996; Liang

et al. 1996; Pomeroy et al. 2007; Oleson et al. 2010; Niu et al. 2011; Clark et al. 2015). Likewise, the need for more realistic hydrological simulations has pushed towards more emphasis on process-based model evaluation (e.g., Gupta et al. 2008, 2009; Martinez and Gupta 2010; Tian et al. 2012; Coron et al. 2014), which is enriched as new observational technologies arise (e.g., Kinar and Pomeroy 2015; McCabe et al. 2017). Further, the community has seen major advances in parameter estimation methods through novel algorithms (e.g., Kavetski et al. 2006; Gharari et al. 2013) and improved objective criteria formulations (e.g., Shafii and Tolson 2015; Beck et al. 2016; Fowler et al. 2018).

9.1.2 Previous Water Balance Characterizations in Chile

The first attempt to estimate annual water balances in South America was led by UNESCO (1982), which proposed a general equation to relate changes in storage (ΔS), precipitation (P), incoming surface runoff (Q_{si}), incoming groundwater fluxes (Q_{gi}), evaporation from water bodies (E), actual evapotranspiration (ET), outgoing surface runoff (Q_{so}), and outgoing groundwater fluxes (Q_{go}) at annual time steps:

$$\Delta S = P + Q_{si} + Q_{gi} - E - ET - Q_{so} - Q_{go} + \eta \tag{9.1}$$

In Eq. (9.1), all terms are expressed in [$L^3\ T^{-1}$], and η represents the estimation error. UNESCO (1982) also recommended to simplify Eq. (9.1) for large areas and very long time periods:

$$\overline{P} - \overline{Q} = \overline{\langle ET \rangle} + \eta \tag{9.2}$$

where $\langle \cdot \rangle$ represents a spatial average, the horizontal bar represents average over time, Q represents the net runoff leaving the basin, and ET stands for all evapotranspiration losses. The proposed approach motivated subsequent applications of Eq. (9.1) over large basins in Central and Southern Chile, neglecting interannual variations in water storage and groundwater runoff (Chilean Water Directorate – DGA 1983a, b, 1984a, 1985). In these studies, unknown fluxes were computed by successive iterations to minimize the error term η, and the results were processed to provide various types of products (e.g., mean annual isohyet and isotherm maps, mean annual ET and annual runoff maps). DGA (1984b) incorporated – for the first time – endorheic basins in water balance estimations across Northern Chile.

These and other studies helped to set a general framework for the current official water balance database, valid for a 30-year period (1951–1980) in continental Chile (DGA 1987). The results presented therein were obtained through Eq. (9.2), setting $Q = 0$ for endorheic basins, estimating ET with Turc's formula, allowing interannual variations in storage ($\Delta S \neq 0$) for arid domains, and a maximum closure error $\eta_{max} = 0.1Q$. The official water balance database has been intensively used as a reference to assess water availability in a myriad of technical applications, including water allocations (See Chaps. 8 and 18).

9.1.3 Aims and Scope of this Chapter

In order to improve and update the official national water balance, DGA (2017) revisited the problem, proposing the use of new datasets and physically-motivated models to improve process understanding. This chapter summarizes the main results from the first three stages of this initiative, whose main goals are: (i) to propose a methodology for updating the national water balance (DGA 2017), (ii) to apply the proposed approach in catchments located in Northern and Central Chile (DGA 2018), and (iii) to apply the proposed approach in catchments located in southern and Austral regions (DGA 2019). The water balance results presented here build upon two key elements:

- A gridded meteorological dataset based on in-situ observations and reanalysis data.
- The calibration and validation of the Variable Infiltration Capacity (VIC) macroscale hydrological model (Wood et al. 1992; Liang et al. 1994) in naturalized catchments across continental Chile.

The following sections describe the proposed modeling framework, the criteria for selecting near-natural catchments, the collection and generation of datasets, and hydrological model descriptions. Then, the results, discussion and perspectives for future work are presented.

9.2 Approach

9.2.1 Study Domain and Basin Selection

A set of near-natural catchments from the CAMELS-CL dataset (Alvarez-Garreton et al. 2018) was used. In CAMELS-CL, the location of DGA streamflow gauges is used to delineate catchment polygons, generate basin-scale time series of hydrometeorological variables, and produce a suite of catchment attributes (topographic, geologic, land cover, climatic, hydrologic and human intervention indices). The main difference between the catchment polygons used here and the BNA catchment boundaries – described in Chap. 8 – (DGA-CIREN 2014) is that the latter do not necessarily match the location of streamflow gauges, and thus cannot be directly used for calibration and validation in hydrologic modelling.

The criterion for selecting near-natural catchments was based on the allocation of water rights. Hence, a maximum threshold value of 5% was adopted for the ratio of annual water volume allocated as permanent consumptive rights to mean annual streamflow (Table 3 in Alvarez-Garreton et al. 2018). In addition, catchments containing large dams were filtered out. From this process, 100 near-natural basins between 18 °S and 55 °S were selected, most of which are located in central and southern Chile. Notwithstanding this, the selected basins feature a wide range of

attributes, including areas spanning 17–27,000 km^2, mean elevations ranging 120–4700 m a.m.s.l., mean slopes varying from 50 to 300 m km^{-1}, and markedly different land cover types (e.g., from completely covered by native forests to completely covered by impervious land). These basin characteristics contain valuable information that can be used for land surface characterization and process representations.

9.2.2 Forcing and Streamflow Data

Characterizing the hydroclimatology of continental Chile is difficult due to many factors, including the diversity and complexity of landscapes across the territory, the major influence of the Andes on spatial precipitation patterns, and the lack of high-altitude ground observations (e.g., Mendoza et al. 2012; Cornwell et al. 2016). Since coherent and homogeneous forcing variables are required for water balance estimates, DGA (2017) introduced the new meteorological dataset CR2MET as part of the national water balance updating project. CR2MET has a 0.05° × 0.05° horizontal resolution and a 3-hour temporal resolution over continental Chile, providing time series of precipitation and daily maximum, mean and minimum temperature for the period 1979–2016. The precipitation product builds upon a statistical downscaling technique that uses topographic descriptors and large-scale variables – such as water vapor fluxes and moisture fluxes – from ERA-Interim (Dee et al. 2011) and ERA5 (Copernicus Climate Change Service (C3S) 2017) as predictors, and daily precipitation records (from stations) as the predictand. A similar approach is used to generate daily maximum and minimum temperature time series, including additional predictors from MODIS land-surface products that provide a better characterization of spatial heterogeneities (e.g., different land cover types). Finally, 3-hourly precipitation and temperature datasets are post-processed from daily-products by adjusting the sub-daily distribution provided by ERA-Interim.

Additional meteorological variables, such as relative humidity and wind speed, were obtained at the CR2MET spatial resolution by interpolating a blend between the ERA-Interim (Dee et al. 2011) and ERA5 (C3S 2017) reanalysis datasets. It should be noted that such blend of products was created since ERA5 was not available for the entire study period (1985–2015) at the moment of data acquisition (early 2018, where only 2010–2016 data were available). However, the updated reanalysis information – despite the short temporal coverage – was included due to several improvements on its development.

Streamflow data were acquired from flow gauges maintained by the DGA – available from the CR2 Climate Explorer (http://explorador.cr2.cl/) – which span varying degrees of data quality and record length. A continuous 4-year record period within 1990–2010 was required from each station to be considered for hydrologic model calibration. If this condition was not met firsthand, we looked into the subperiods 1985–1990 and 2010–2015. Once the minimum record length requirement was met, all the information available was used in the calibration process. Figure 9.1

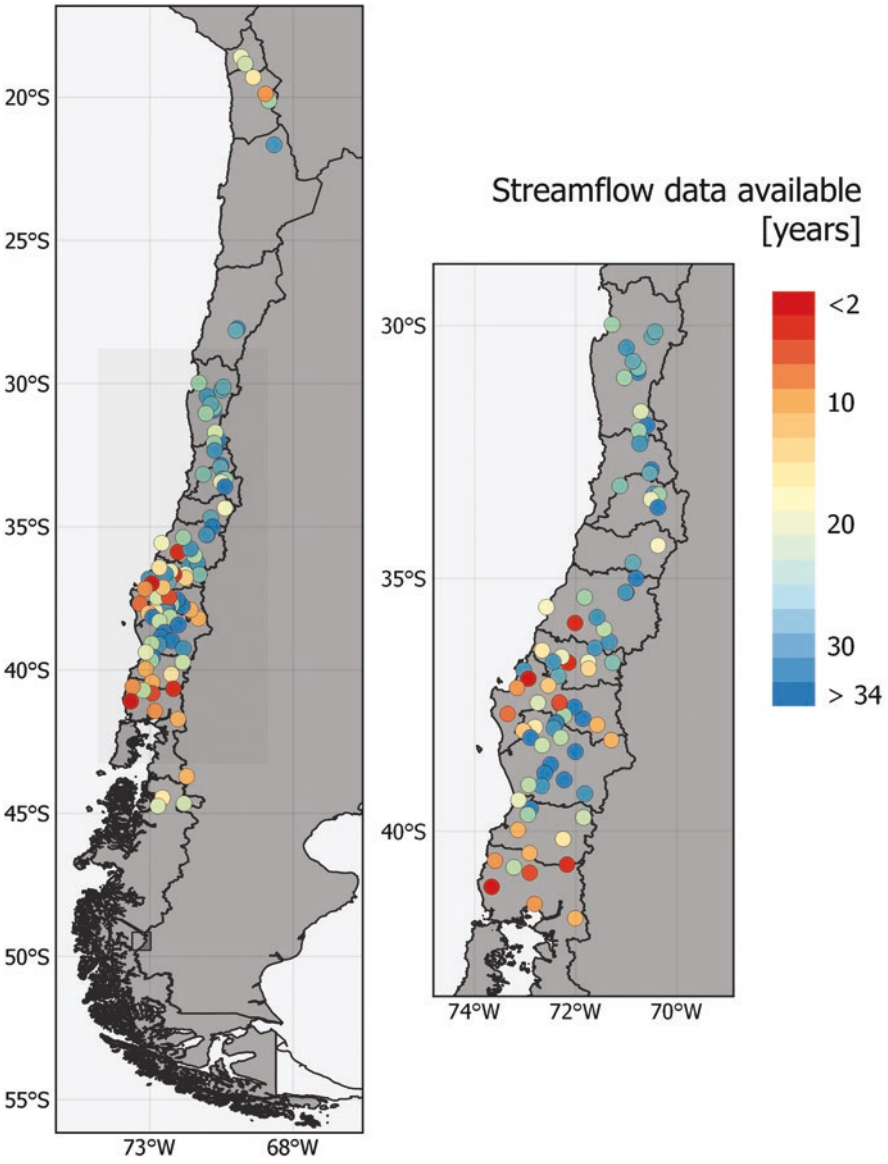

Fig. 9.1 Location of streamflow stations and data availability for selected 'near-natural' basins

shows the location of the stations that met such requirement and the number of water years with available data. It is noteworthy that most of the stations are located between 30°S and 45°S, where most of the population lives and economic activities take place. A few streamflow gauges are located northern than 30°S due to the small number of prevailing water courses in a domain with dry climatic conditions (as shown in Chap. 2).

Table 9.1 List of VIC parameters calibrated

N°	Parameter	Description
1	infilt	Variable infiltration curve parameter (binfilt)
2	D_s	Fraction of Ds_{max} where non-linear baseflow begins
3	Ds_{max}	Maximum velocity (mm day^{-1}) of baseflow
4	W_s	Fraction of maximum soil moisture where non-linear baseflow occurs
5	C	Exponent used in baseflow curve
6	$depth_1$	Thickness (m) of each soil moisture layer
7	$depth_2$	
8	$depth_3$	
9	K_{sat}	Saturated hydrologic conductivity (mm day^{-1})
10	New_{alb}	Fresh snow albedo
11	Alb_{acum_a}	Snow albedo curve parameter
12	Alb_{thaw_a}	Snow albedo curve parameter
13	T_{rain}	Minimum temperature (°C) for rainfall occurrence
14	r_{snow}	Snow surface roughness (m)

9.2.3 Hydrological Modeling

The Variable Infiltration Capacity model (VIC, Liang et al. 1994), a physically-motivated, distributed hydrological model that resolves mass and energy balances, was configured for this study. In VIC, each grid cell can have up to three soil layers and multiple land cover types. Two soil layers represent the interaction between moisture and vegetation, and the bottom soil layer is used to simulate baseflow processes. Snowpack dynamics are simulated by a two-layer mass and energy balance model (Cherkauer and Lettenmaier 2003; Andreadis et al. 2009), where the surface layer solves the energy balance between the snowpack and the atmosphere, and the lower layer stores the excess snow mass from the thin upper surface layer.

The updated water balance considers the standard three-layer soil implementation, with up to nine different land cover classes, a 0.05° × 0.05° horizontal resolution, and 3-hour simulation time steps. The calibration process involves 14 parameters (Table 9.1) using the Shuffled Complex Evolution (SCE-UA; Duan et al. 1993) algorithm, and a 3-year warm-up period before computing performance metrics. The Kling-Gupta efficiency (KGE) criterion (Gupta et al. 2009) evaluated over daily streamflow time series was used as objective function:

$$KGE = 1 - \sqrt{(r-1)^2 + (\beta-1)^2 + (\gamma-1)^2} \tag{9.3}$$

Where r is the linear correlation coefficient between simulated and observed flows, β is the ratio of the mean of simulated flows, μ_s, to the mean of observed flow, μ_o, and γ is the ratio of the standard deviation of simulated flows, σ_s, to the standard

deviation of observed flows, σ_o. Streamflow simulations were also assessed through the Nash-Sutcliffe efficiency (NSE; Nash and Sutcliffe 1970). Finally, modeled fractional snow-covered area (fSCA) and snow water equivalent (SWE) were contrasted against MODIS fSCA and SWE from the Cortés and Margulis (2017) dataset to identify biases in mountainous precipitation, threshold snow and rain temperature, and snow surface roughness (T_{rain} and r_{snow} in Table 9.1, respectively).

9.3 Water Balance Results

9.3.1 Assessment of CR2MET Products

Figure 9.2 depicts observed and modeled (i.e., CR2MET) climatological mean annual values for precipitation and maximum temperature for the period 1979–2016. Both estimations and observations follow similar spatial distributions. The zoom-in panels for each variable illustrate the level of detail achieved in CR2MET products due to the use of 5-km topographic information. Further, the orographic effect of the Andes Cordillera plays a fundamental role in Northern and Central Chile (Fig. 9.3), with the smallest precipitation amounts near the coast. The opposite spatial pattern is observed in the Southern region (bottom panel in Fig. 9.3), where larger precipitation amounts are observed near the coastline due to prevailing westerly winds (Garreaud 2009).

A leave-one-out cross-validation procedure was conducted to assess the quality of CR2MET products. Figure 9.4 compares the seasonal behavior of observed and

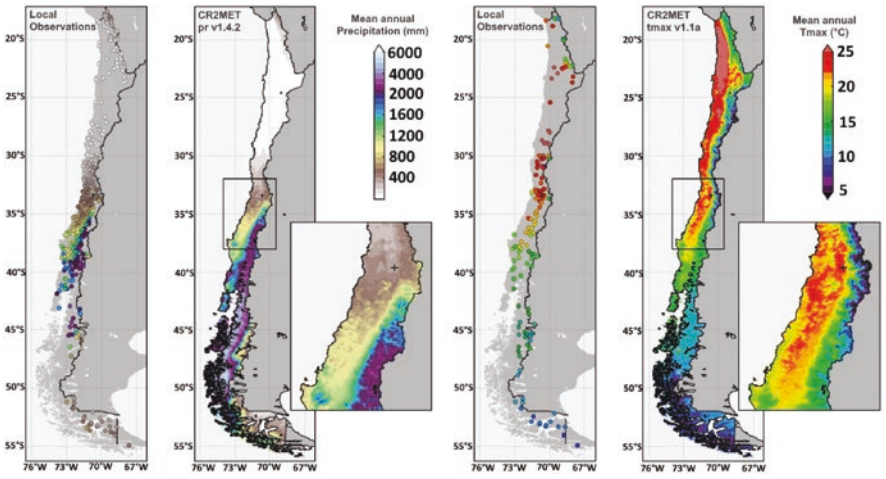

Fig. 9.2 Climatological mean values (1979–2016) for (left) annual precipitation and (right) annual maximum daily temperature. Maps with points show observed values in measuring stations, whereas maps with continuous coloring show the CR2MET estimated values for the same period

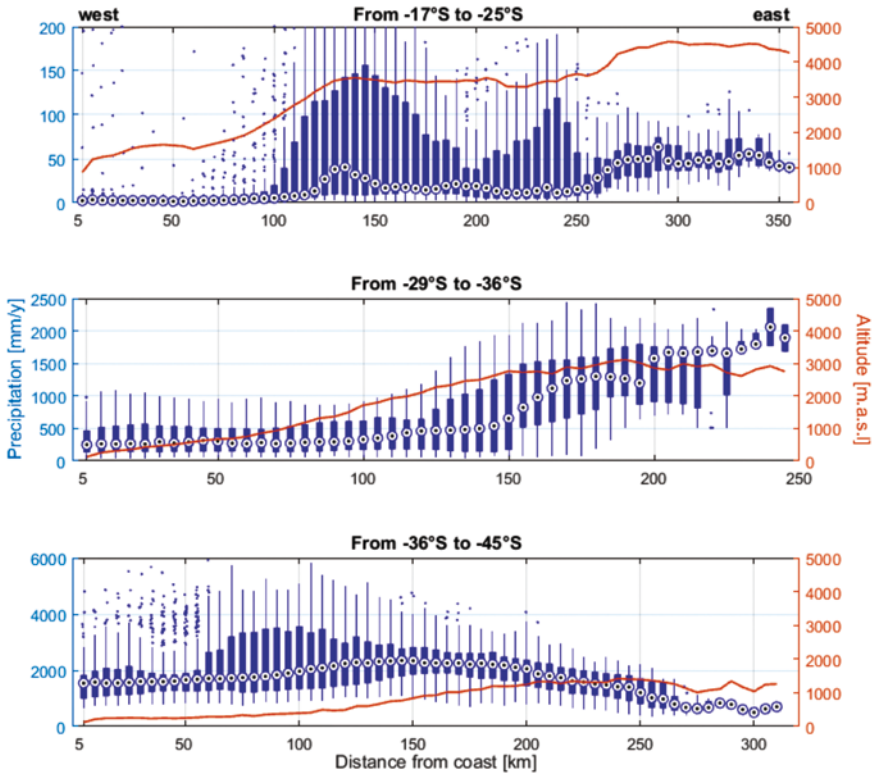

Fig. 9.3 Mean annual precipitation versus distance from the coastline for grid cells located at three different latitudinal regions (blue boxplots). Each boxplot shows the median as white circles inside the box, the interquartile range (difference between the 25th and 75th percentiles) as the length of the box, and outliers as blue dots. The red line represents terrain elevation (secondary axis)

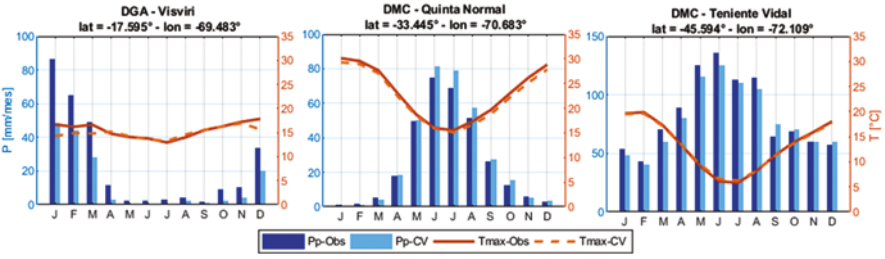

Fig. 9.4 Comparison between observations (Obs) and cross-validated estimations (CV) for mean monthly precipitation (P) and maximum temperature (Tmax) at three sites: (left) Visviri, (center) Quinta Normal, and (c) Teniente Vidal

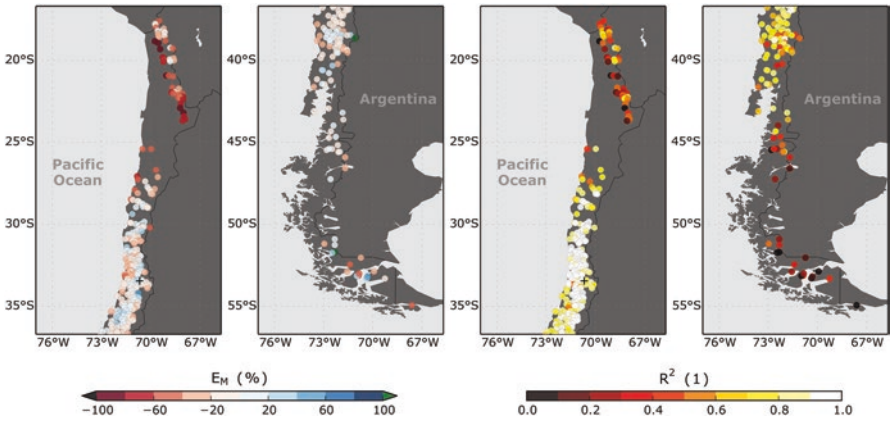

Fig. 9.5 Cross-validation performance metrics for daily precipitation estimates (1979–2015). (Left) Percent bias (E_M), and (right) coefficient of determination (R^2)

estimated monthly precipitation and maximum temperature at three stations located in the Altiplano (DGA-Visviri), Central Chile (DMC-Quinta Normal) and the Patagonian area (DMC-Teniente Vidal). These stations are good examples of the diverse climatic conditions within the study area, including summer Altiplano monsoons (Visviri), Mediterranean climate (Quinta Normal), and Oceanic climate (Teniente Vidal). Overall, seasonal cycles are well reproduced, although both climatic variables in Northern stations remain the hardest to accurately estimate.

Figure 9.5 shows the spatial distribution of two metrics – percent bias and coefficient of determination (R^2) – for cross-validated daily precipitation estimates (1979–2015). Overall, larger biases and lower R^2 values are estimated at the northernmost stations (Altiplanic region). Because of the low annual precipitations (Fig. 9.2), estimates of this variable across northern stations can yield relatively large biases. Similarly, low performance metrics are obtained for the far south region, where values of $R^2 < 0.2$ are observed. Inter-region differences in the accuracy of CR2MET estimates can be partly attributed to the heterogeneous distribution of meteorological stations across the country, i.e., the scant number of stations at the Altiplano and Patagonia regions impairs the development of robust regression equations. Conversely, higher R^2 values are obtained in Central Chile, since excluding one station barely affects the model training process.

9.3.2 Individual Basin Calibration

Figure 9.6 displays model calibration results across the study domain. Although a relatively homogeneous spatial distribution of daily KGE is achieved (upper left panel in Fig. 9.6), considerable differences in NSE are observed between Northern and Central-Southern catchments (upper right panel in Fig. 9.6). In the latter group, a better model performance is obtained because snow processes – a dominant control in

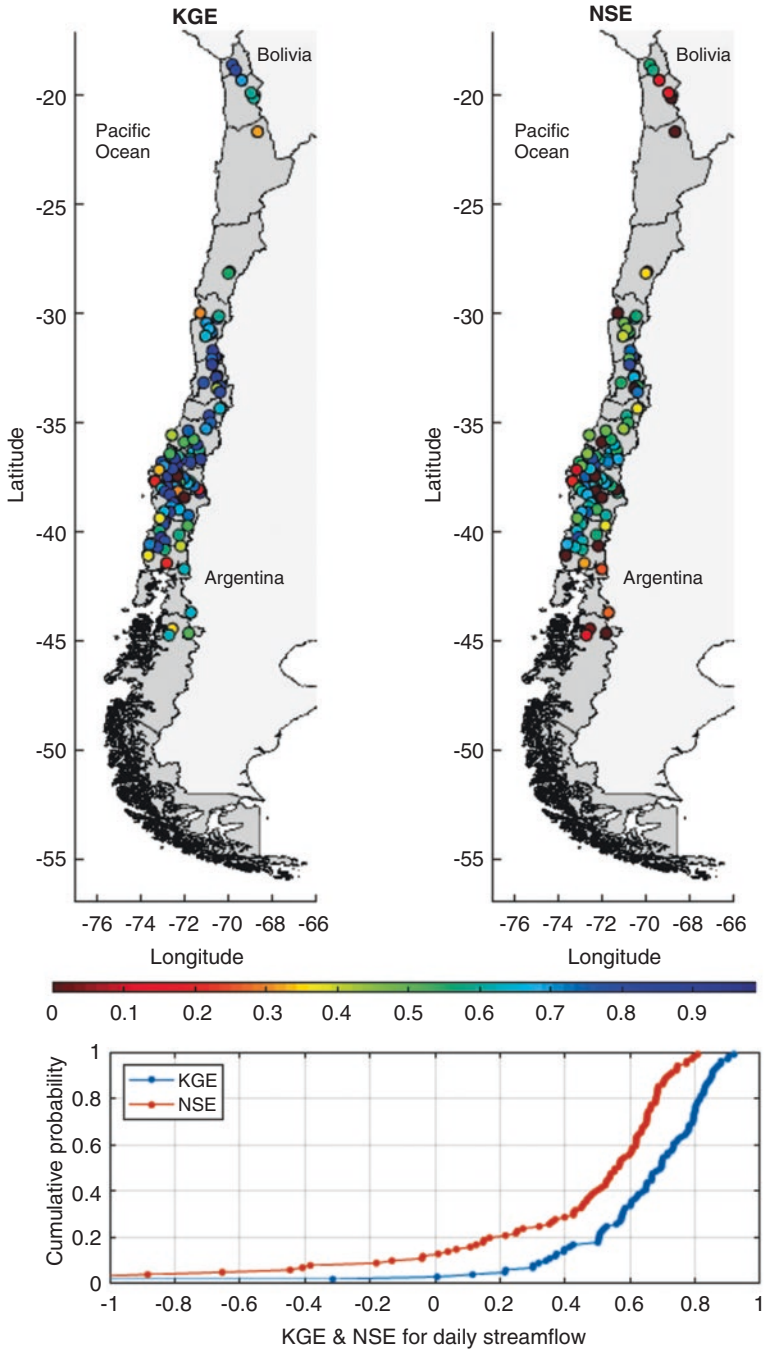

Fig. 9.6 Performance of daily streamflow simulations: (upper-left) KGE, (upper-right) NSE, and (bottom) cumulative probability distributions for calibrated basins in natural regime

the hydrology of this region – are well represented in VIC. On the other hand, northern basins are dominated by groundwater contributions throughout the year, with occasional flashfloods occurring between December and February due to Altiplano heavy rainfall events. Groundwater modeling remains a difficult task in this region because surface basin boundaries do not necessarily match groundwater drainage boundaries (Montgomery et al. 2003). Furthermore, VIC does not include aquifers nor horizontal connectivity between grid cells, missing relevant process representations in arid catchments. Such structural deficiency has already been noticed and demonstrated in other study domains (e.g., Demaria et al. 2007; Newman et al. 2017).

Despite the above issues, and according to the criteria proposed by Moriasi et al. (2007), model performance is "very good" in 40% of the catchments in terms of KGE (values above 0.75, Fig. 9.6), whereas in 60% of the basins the performance is "good" (values above 0.65), while 80% provide "satisfactory" scores (values above 0.5). NSE values are lower than KGE, which is expected as calibration focused on the latter score.

9.3.3 Annual Water Balance

During the analysis period (1985–2015), the partitioning of precipitation into evapotranspiration and runoff (Q) shows dependency with latitude (Fig. 9.7). Such relationship can be attributed to variations in available solar energy that modulates evapotranspiration processes, and the spatial variability of precipitation across continental Chile. In Northern catchments, the influence of convective storms is stronger than in Central Chile, where frontal systems explain most of annual precipitation (Garreaud 2009). In the Altiplano region, more than 90% of annual precipitation (P) becomes evapotranspiration (ET) (Fig. 9.7), while ET/P is less than 10% in some basins located in Southern Chile.

In terms of water budget, considerable spatial variations in climatological runoff ratios and evapotranspiration ratios (1985–2015 period) are observed (Fig. 9.7).

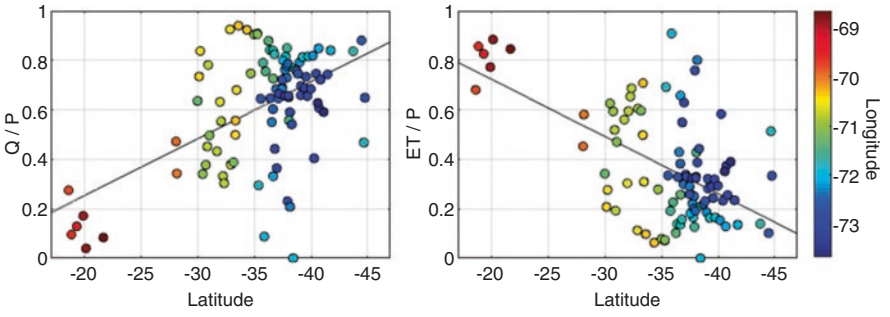

Fig. 9.7 Latitudinal and longitudinal variations at the catchment-scale (left) annual runoff ratio Q/P, and (right) evapotranspiration ratio ET/P across the study domain

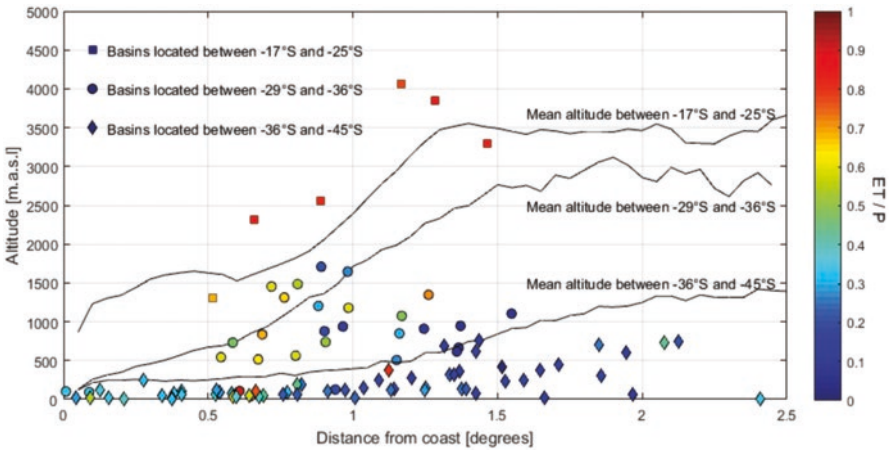

Fig. 9.8 Mean altitude and spatial variation of ET/P ratios at three different latitudinal domains: (i) northern region (17°–25° S); (ii) central region (29°–36° S; and southern region, between 36° and 45° S)

Northern and Andean catchments are very arid, and most precipitation (~70%) evapotranspirates to the atmosphere. Detailed analyses of longitudinal cross sections (northern, central and southern latitudes, Fig. 9.8) reveal that the largest evapotranspiration demands occur in Northern high-elevation catchments, with a decrease towards the coast due to lower atmospheric moisture in the Pacific Ocean (Fig. 9.8). Central and Southern regions show larger spatial heterogeneities, with no clear trend in water budget components, except in the southern region where the influence of the ocean results in decreased ET/P ratios towards the coast.

9.3.4 Seasonal Water Balance

To examine differences in seasonal hydrologic behavior among basins, the catchments were classified based on meteorological data using the Autoclass-C software (Cheeseman and Stutz 1996; Sawicz et al. 2011). Three climatic descriptors were included in the classification process: precipitation seasonality (p-seasonality, Woods 2009; Addor et al. 2017; Alvarez-Garreton et al. 2018), fraction of snow events (snow-frac) and aridity index. The above indices were computed for each 0.05° × 0.05° grid cell – as defined in the CR2MET dataset – and then spatially averaged within the catchments' boundaries. As a result, four clusters of catchments were identified (markers in Fig. 9.9, right panel), with differences in seasonal water balance, illustrated as mean monthly variations in precipitation, runoff, evapotranspiration and water storage – calculated as the sum of model states – following the Wundt's Diagram (Wundt 1953). The first group (star marker) belongs to the Altiplano region, where precipitation occurs between December to March due to the

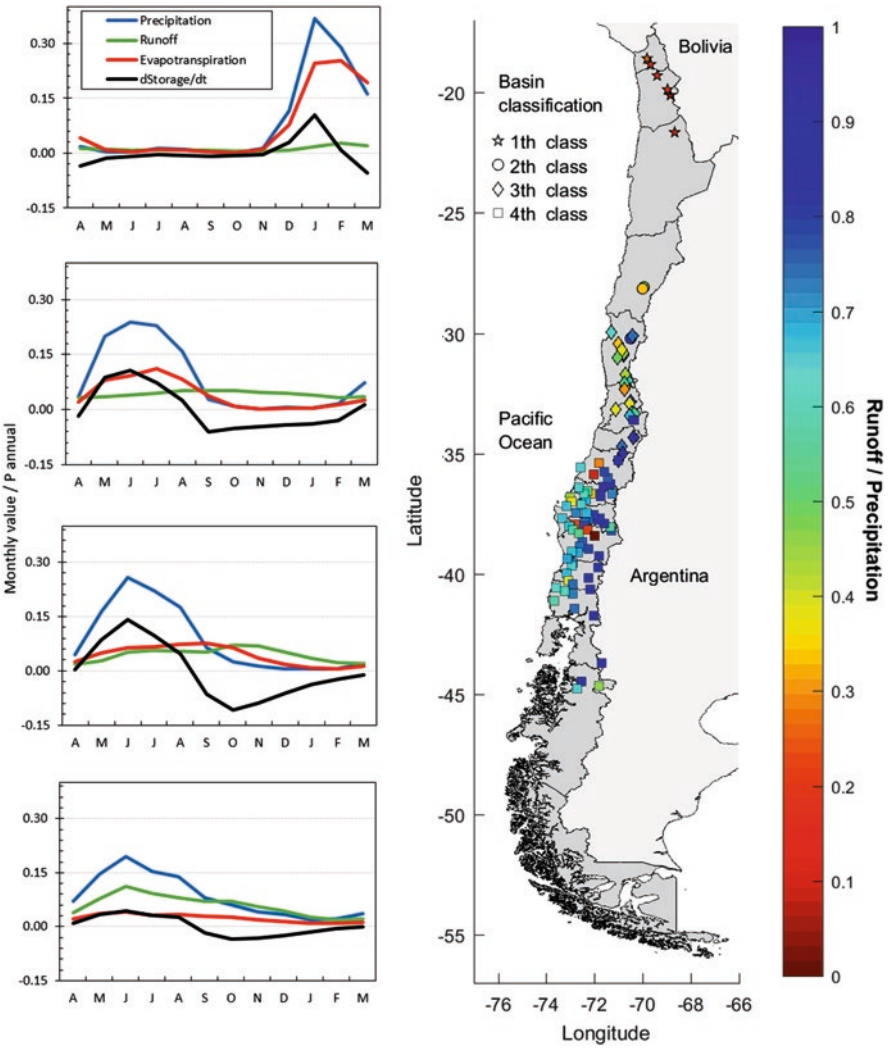

Fig. 9.9 (*Left*) Average monthly water balance components (normalized by annual precipitation) and (*right*) runoff coefficients during 1985–2015, for the basin types 1 to 4 (displayed from top to bottom along the left panels) obtained from the climate-based catchment classification. Different symbols in the right panel represent different catchment types

South American Monsoon (Garreaud 2009), activating evapotranspiration and runoff fluxes within the same season (left panel in Fig. 9.9). In these catchments, there is an important water storage component and the main flux is evapotranspiration, while runoff ratio is less than 10%. Most of northern-central basins (29°S–35°S) located in the Andes Cordillera have a strong dependency on snow accumulation and melting processes (circle and diamond markers in left panel of Fig. 9.9).

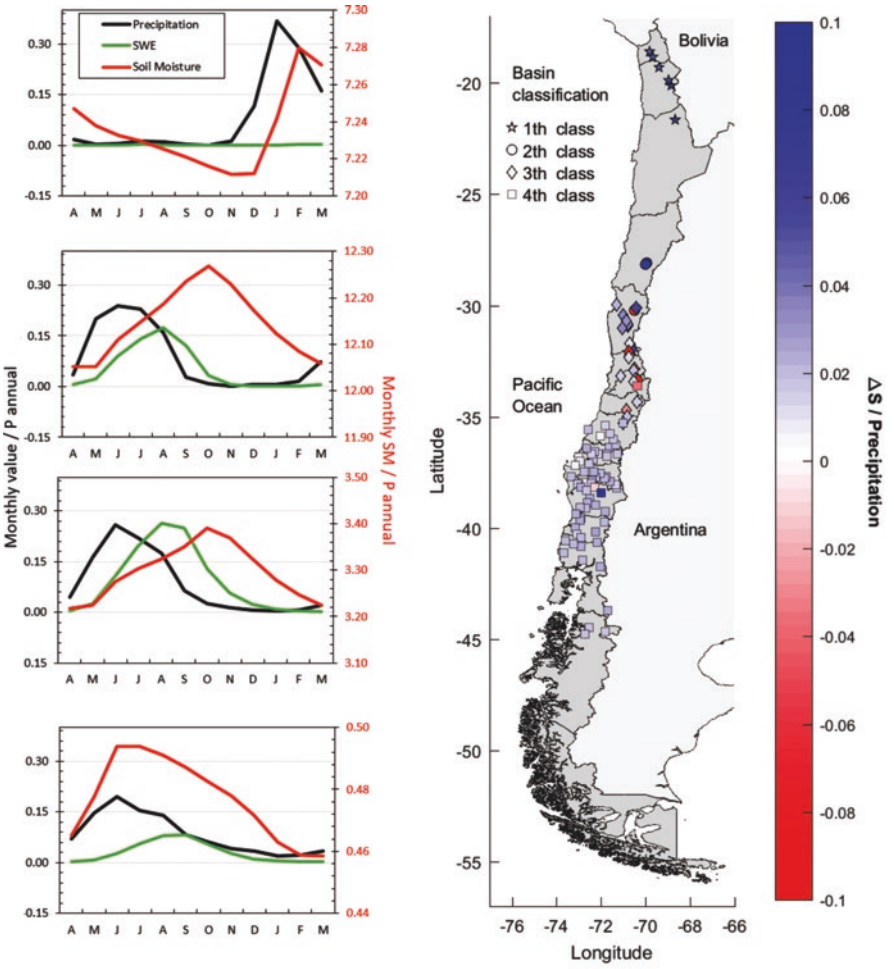

Fig. 9.10 (*Left*) Average mean monthly soil moisture (SM), SWE and (*right*) annual variations in total basin storage (normalized by mean annual precipitation) during 1985–2015, for the basin types 1 to 4 (displayed from top to bottom along the left panels) obtained from the climate-based catchment classification. Different symbols in the right panel represent different catchment types

Snowmelt typically begins in late September, at the beginning of the spring season, and the water stored as snow and soil moisture is released during spring and summer, respectively (Fig. 9.10). Evapotranspiration in northern basins (28°S–30°S, circle markers) depends on the water available from precipitation, while snow sublimation becomes a relevant water balance control in catchments located in Central Chile (diamond markers). Southern basins (square markers) are rainfall-dominated, with the largest amounts recorded in winter and a weaker influence of snow processes on the seasonal water balance. Therefore, the largest (smallest) runoff

volumes are observed in winter (summer), as the water stored in the soil is released. Finally, variations in total storage during 1985–2015 are less than 5% of the mean annual precipitation in most catchments (Fig. 9.10).

9.4 Discussion

Quantifying natural water resources in continental Chile is a challenging task, given the large physiographic, climatic and hydrological heterogeneities across the territory. This chapter depicts the main results from an ongoing, interdisciplinary effort to update the national water balance database (DGA 2017). The results presented here build upon hydrological model simulations conducted with the Variable Infiltration Capacity (VIC) model, using datasets that characterize climate (CR2MET) and catchment attributes (CAMELS-CL) in continental Chile.

CR2MET represents a milestone in the development of meteorological information for scarce data regions, especially in the arid Northern regions, high Andean mountains and Patagonia. Overall, CR2MET provides reliable precipitation and temperature estimates at annual and seasonal time scales. Due to higher density of stations in Central Chile (−30 to −40°S), the accuracy of CR2MET products is larger (i.e., higher R^2 and lower biases) within this sub-domain. Similarly, the CAMELS-CL database is the first harmonized compilation of basin attributes and hydrometeorological time series at the catchment scale for continental Chile, with the novel contribution of human intervention descriptors. Therefore, 'near-natural' catchments can be identified and used for detailed process-based studies using hydrological models.

In general, good calibration results are obtained in terms of KGE and NSE scores, excepting arid catchments (Northern Chile) due to model structural deficiencies – specifically, the lack of aquifer representation and lateral connectivity between modeling units. The water balance analysis shows a large spatial heterogeneity in precipitation partitioning, with 90% becoming evapotranspiration in the Altiplano region whereas in Southern Chile the runoff ratio is greater than 80%. Although no clear dependencies with latitude are found, a strong relationship with longitude is obtained in central and southern Chile, with higher ET/P values near the coast and lower values as one approaches the Andes Cordillera.

The climate-based classification – conducted for 'near natural' basins – provides four groups of basins with different hydrological behavior:

- Basins in the Altiplano region, with precipitation and runoff peaks during summer (i.e., January–March) and high ET/P values.
- Northern-central basins with headwaters in the Andes Cordillera, where most ET occurs during winter (April–September).
- Mountain basins in Central Chile, where runoff peaks during spring and summer (i.e., October–March), and the largest ET values are observed during the spring season (i.e., October–December). In these basins, ET is decoupled with P due to

snowpack presence (which provides water availability) and increased incoming energy.
- Southern catchments, where precipitation and peak runoff occur during winter (i.e., April–September).

Despite outstanding advances in hydrological modeling tools and new climate and catchment datasets, developing robust methods for water balance estimates in ungauged basins remains a critical challenge. Indeed, the area covered by all the basins included in this study represents only 17% of continental Chile. Future work will expand water balance estimates to the rest of the territory through the implementation of parameter regionalization techniques, and will include projections of climate change impacts on relevant fluxes and storages.

References

Addor N, Rössler O, Köplin N et al (2014) Robust changes and sources of uncertainty in the projected hydrological regimes of Swiss catchments. Water Resour Res 50:7541–7562. https://doi.org/10.1002/2014WR015549

Addor N, Newman AJ, Mizukami N, Clark MP (2017) The CAMELS data set: catchment attributes and meteorology for large-sample studies. Hydrol Earth Syst Sci. https://doi.org/10.5194/hess-21-5293-2017

Alvarez-Garreton C, Mendoza PA, Boisier JP et al (2018) The CAMELS-CL dataset: catchment attributes and meteorology for large sample studies – Chile dataset. Hydrol Earth Syst Sci 22:5817–5846. https://doi.org/10.5194/hess-22-5817-2018

Andreadis KM, Storck P, Lettenmaier DP (2009) Modeling snow accumulation and ablation processes in forested environments. Water Resour Res 45:W05429. https://doi.org/10.1029/2008WR007042

Andréassian V, Hall A, Chahinian N, Schaake J (2006) Why should hydrologists work on a large number of basin data sets? In: Large Sample Basin experiments for hydrological model parameterization. Results of the model parameter experiment – MOPEX, vol 307. IAHS Publication, Wallingford, pp 1–5

Beck HE, van Dijk AIJM, de Roo A et al (2016) Global-scale regionalization of hydrologic model parameters. Water Resour Res 52:3599–3622. https://doi.org/10.1002/2015WR018247

Berghuijs WR, Sivapalan M, R a W, Savenije HHG (2014) Patterns of similarity of seasonal water balances: a window into streamflow variability over a range of time scales. Water Resour Res 50:5638–5661. https://doi.org/10.1002/2014WR015692

Blöschl G, Montanari A (2010) Climate change impacts – throwing the dice? Hydrol Process 24:374–381. https://doi.org/10.1002/hyp.7574

Carmona AM, Sivapalan M, Yaeger MA, Poveda G (2014) Regional patterns of interannual variability of catchment water balances across the continental U.S.: a Budyko framework. Water Resour Res 50:9177–9193. https://doi.org/10.1002/2014WR016013

Cheeseman P, Stutz J (1996) Bayesian cassification (AutoClass): theory and results. In: Advances in knowledge discovery and data mining. AAAI, Menlo Park

Chen F, Mitchell K, Schaake J et al (1996) Modeling of land surface evaporation by four schemes and comparison with FIFE observations. J Geophys Res Atmos 101:7251–7268

Cherkauer KA, Lettenmaier DP (2003) Simulation of spatial variability in snow and frozen soil. J Geophys Res 108:8858. https://doi.org/10.1029/2003JD003575

Clark MP, Nijssen B, Lundquist JD et al (2015) A unified approach for process-based hydrologic modeling: 1. Modeling concept. Water Resour Res. https://doi.org/10.1002/2015WR017198

Clark MP, Wilby RL, Gutmann ED et al (2016) Characterizing uncertainty of the hydrologic impacts of climate change. Curr Clim Chang Rep 2:55–64. https://doi.org/10.1007/s40641-016-0034-x
Copernicus Climate Change Service (C3S) (2017) ERA5: fifth generation of ECMWF atmospheric reanalyses of the global climate. In: Copernicus Climate Change Service Climate Data Store
Cornwell E, Molotch NP, McPhee J (2016) Spatio-temporal variability of snow water equivalent in the extra-tropical Andes cordillera from distributed energy balance modeling and remotely sensed snow cover. Hydrol Earth Syst Sci 20:411–430. https://doi.org/10.5194/hess-20-411-2016
Coron L, Andréassian V, Perrin C et al (2014) On the lack of robustness of hydrologic models regarding water balance simulation: a diagnostic approach applied to three models of increasing complexity on 20 mountainous catchments. Hydrol Earth Syst Sci 18:727–746. https://doi.org/10.5194/hess-18-727-2014
Cortés G, Margulis S (2017) Impacts of El Niño and La Niña on interannual snow accumulation in the Andes: Results from a high-resolution 31 year reanalysis. Geophys Res Lett 44:6859–6867. https://doi.org/10.1002/2017GL073826
Dee DP, Uppala SM, Simmons AJ et al (2011) The ERA-interim reanalysis: configuration and performance of the data assimilation system. Q J R Meteorol Soc 137:553–597. https://doi.org/10.1002/qj.828
Demaria EM, Nijssen B, Wagener T (2007) Monte Carlo sensitivity analysis of land surface parameters using the variable infiltration capacity model. J Geophys Res 112:1–15. https://doi.org/10.1029/2006JD007534
DGA (1983a) Balance hidrológico nacional regiones V, VI, VII y Metropolitana. Santiago de Chile
DGA (1983b) Balance Hídrico Nacional. Regiones VIII, IX y X. Santiago de Chile
DGA (1984a) Balance Hidrológico Nacional XI Región. Santiago de Chile
DGA (1984b) Balance hidrológico nacional regiones III y IV. Santiago de Chile
DGA (1985) Balance hidrológico nacional Cuenca del Rio Itata. Santiago de Chile
DGA (1987) Balance hídrico de Chile
DGA (2017) Metodología para la Actualización del Balance Hídrico Nacional
DGA (2018) Aplicación de La Metodología de Actualización del Balance Hídrico Nacional en las Cuencas de la Macrozona Norte y Centro
DGA (2019) Aplicación de La Metodología de Actualización del Balance Hídrico Nacional en las Cuencas de la Macrozona Sur y Parte de la Macrozona Austral
DGA-CIREN (2014) Redefinición de la clasificación red hidrográfica a nivel Nacional
Duan QY, Gupta VK, Sorooshian S (1993) Shuffled complex evolution approach for effective and efficient global minimization. J Optim Theory Appl 76:501–521. https://doi.org/10.1007/BF00939380
Fowler K, Peel M, Western A, Zhang L (2018) Improved rainfall-runoff calibration for drying climate: choice of objective function. Water Resour Res 54:3392–3408. https://doi.org/10.1029/2017WR022466
Garreaud R (2009) Advances in geosciences the Andes climate and weather. Adv Geosci 7:9. https://doi.org/10.5194/adgeo-22-3-2009
Gharari S, Hrachowitz M, Fenicia F, Savenije HHG (2013) An approach to identify time consistent model parameters: sub-period calibration. Hydrol Earth Syst Sci 17:149–161. https://doi.org/10.5194/hess-17-149-2013
Gupta HV, Wagener T, Liu Y (2008) Reconciling theory with observations : elements of a diagnostic approach to model evaluation. Hydrol Process 22:3802–3813. https://doi.org/10.1002/hyp
Gupta HV, Kling H, Yilmaz KK, Martinez GF (2009) Decomposition of the mean squared error and NSE performance criteria: implications for improving hydrological modelling. J Hydrol 377:80–91. https://doi.org/10.1016/j.jhydrol.2009.08.003
Gupta HV, Perrin C, Blöschl G et al (2014) Large-sample hydrology: a need to balance depth with breadth. Hydrol Earth Syst Sci 18:463–477. https://doi.org/10.5194/hess-18-463-2014
Hrachowitz M, Savenije HHG, Blöschl G et al (2013) A decade of predictions in ungauged basins (PUB)—a review. Hydrol Sci J 58:1198–1255. https://doi.org/10.1080/02626667.2013.803183

Huntington TG (2006) Evidence for intensification of the global water cycle: review and synthesis. J Hydrol 319:83–95. https://doi.org/10.1016/j.jhydrol.2005.07.003

IPCC (2013) Climate change 2013: the physical science basis. Contribution of working group I to the fifth assessment report of the intergovernmental panel on climate change. Cambridge University Press, Cambridge/New York

Kavetski D, Kuczera G, Franks SW (2006) Calibration of conceptual hydrological models revisited: 2. Improving optimisation and analysis. J Hydrol 320:187–201. https://doi.org/10.1016/j.jhydrol.2005.07.013

Kinar NJ, Pomeroy JW (2015) Measurement of the physical properties of the snowpack. Rev Geophys 53:481–544. https://doi.org/10.1002/2015RG000481

Liang X, Lettenmaier DP, Wood EF, Burges SJ (1994) A simple hydrologically based model of land surface water and energy fluxes for general circulation models. J Geophys Res 99:14,415.14.428

Liang X, Wood EF, Lettenmaier DP (1996) Surface soil moisture parameterization of the VIC-2L model: evaluation and modification. Glob Planet Chang 13:195–206. https://doi.org/10.1016/0921-8181(95)00046-1

Martinez GF, Gupta HV (2010) Toward improved identification of hydrological models: a diagnostic evaluation of the " abcd " monthly water balance model for the conterminous United States. Water Resour Res 46:W08507. https://doi.org/10.1029/2009WR008294

McCabe MR, Alsdorf DE, Miralles DG et al (2017) The future of earth observation in hydrology. Hydrology and earth system sciences (under review). Hydrol Earth Syst Sci:3879–3914

Mendoza PA, McPhee J, Vargas X (2012) Uncertainty in flood forecasting: a distributed modeling approach in a sparse data catchment. Water Resour Res 48:W09532. https://doi.org/10.1029/2011WR011089

Mendoza PA, Clark MP, Mizukami N et al (2016) How do hydrologic modeling decisions affect the portrayal of climate change impacts? Hydrol Process 30:1071–1095. https://doi.org/10.1002/hyp.10684

Milly PCD, Dunne KA, Vecchia AV (2005) Global pattern of trends in streamflow and water availability in a changing climate. Nature 438:347–350. https://doi.org/10.1038/nature04312

Milly PCD, Betancourt J, Falkenmark M et al (2008) Stationarity is dead: whither water management? Science 319:573–574. https://doi.org/10.1126/science.1151915

Mizukami N, Clark MP, Gutmann ED et al (2016) Implications of the methodological choices for hydrologic portrayals of climate change over the contiguous United States: statistically downscaled forcing data and hydrologic models. J Hydrometeorol 17:73–98. https://doi.org/10.1175/JHM-D-14-0187.1

Montgomery EL, Rosko MJ, Castro SO et al (2003) Interbasin underflow between closed altiplano basins in Chile. Ground Water. https://doi.org/10.1111/j.1745-6584.2003.tb02386.x

Moriasi DN, Arnold JG, Van Liew MW et al (2007) Model evaluation guidelines for systematic quantification of accuracy in watershed simulations. Trans ASABE. https://doi.org/10.13031/2013.23153

Müller Schmied H, Adam L, Eisner S et al (2016) Impact of climate forcing uncertainty and human water use on global and continental water balance components. Proc Int Assoc Hydrol Sci 374:53–62. https://doi.org/10.5194/piahs-374-53-2016

Nash JE, Sutcliffe JV (1970) River flow forecasting through conceptual models part I — a discussion of principles. J Hydrol 10:282–290. https://doi.org/10.1016/0022-1694(70)90255-6

Newman AJ, Mizukami N, Clark MP et al (2017) Benchmarking of a physically based hydrologic model. J Hydrometeorol 18:2215–2225. https://doi.org/10.1175/JHM-D-16-0284.1

Niu G-Y, Yang Z-L, Mitchell KE et al (2011) The community Noah land surface model with multiparameterization options (Noah-MP): 1. Model description and evaluation with local-scale measurements. J Geophys Res 116:D12109. https://doi.org/10.1029/2010JD015139

Oleson KW, Lawrence DM, Gordon B, et al (2010) Technical Description of version 4.0 of the Community Land Model (CLM). Boulder, Colorado, USA.

Parajka J, Merz R, Blöschl G (2007) Uncertainty and multiple objective calibration in regional water balance modelling: case study in 320 Austrian catchments. Hydrol Process 21:435–446. https://doi.org/10.1002/hyp.6253

Pomeroy JW, Gray DM, Brown T et al (2007) The cold regions hydrological model : a platform for basing process representation and model structure on physical evidence. Hydrol Process 21:2650–2667. https://doi.org/10.1002/hyp

Sankarasubramanian A, Vogel RM (2002) Annual hydroclimatology of the United States. Water Resour Res 38.:19-1-19–12. https://doi.org/10.1029/2001WR000619

Sawicz K, Wagener T, Sivapalan M et al (2011) Catchment classification: empirical analysis of hydrologic similarity based on catchment function in the eastern USA. Hydrol Earth Syst Sci 15:2895–2911. https://doi.org/10.5194/hess-15-2895-2011

Shafii M, Tolson BA (2015) Optimizing hydrological consistency by incorporating hydrological signatures into model calibration objectives. Water Resour Res 51:3796–3814. https://doi.org/10.1002/2014WR016520

Sivapalan M (2018) From engineering hydrology to earth system science: milestones in the transformation of hydrologic science. Hydrol Earth Syst Sci 22:1665–1693. https://doi.org/10.5194/hess-22-1665-2018

Tian F, Li H, Sivapalan M (2012) Model diagnostic analysis of seasonal switching of runoff generation mechanisms in the Blue River basin, Oklahoma. J Hydrol 418–419:136–149. https://doi.org/10.1016/j.jhydrol.2010.03.011

Tian S, Tregoning P, Renzullo LJ et al (2017) Improved water balance component estimates through joint assimilation of GRACE water storage and SMOS soil moisture retrievals. Water Resour Res 53:1820–1840. https://doi.org/10.1002/2016WR019641

UNESCO (1982) Guía Metodológica para la elaboración del Balance Hídrico de América del Sur. Montevideo, Uruguay

Vandewiele GL, Elias A (1995) Monthly water balance of ungauged catchments obtained by geographical regionalization. J Hydrol 170:277–291. https://doi.org/10.1016/0022-1694(95)02681-E

Wigmosta M, Vail L, Lettenmaier D (1994) A distributed hydrology-vegetation model for complex terrain. Water Resour Res 30:1665–1679

Wood EF, Lettenmaier DP, Zartarian VG (1992) A land-surface hydrology parameterization with subgrid variability for general circulation models. J Geophys Res 97:2717–2728. https://doi.org/10.1029/91JD01786

Woods RA (2009) Analytical model of seasonal climate impacts on snow hydrology: continuous snowpacks. Adv Water Resour. https://doi.org/10.1016/j.advwatres.2009.06.011

Wundt W (1953) Gewässerkunde. Springer, Berlin